MCR/14

Met O 11 Technical Note No 199

The impact of data from the HERMES system on the fine mesh data assimilation scheme - a case study.

by

R.S. Bell and O. Hammon

February 1985

Note

This paper has not been published. Permission to quote from it should be obtained from the Assistant Director of the above Meteorological Office Branch.

Contents

The impact of data from the HERMES System on the fine mesh data assimilation scheme - a case study.

by R.S. Bell and O. Hammon

1. Introduction

One of the more important aspects of the work of the Central Forecast Office is the provision of forecast guidance for the whole of the United Kingdom for 24 hours ahead. The fine mesh version of the 15-level numerical model of the atmosphere which was introduced in December 1982 plays an important part in this process. The problems of short-range weather forecasting and interpretation of numerical model products have recently been described by Woodroffe (1984). The success of a numerical model depends on several factors. The sophistication of the model and how well the physical processes are parametrised is undoubtedly important but perhaps just as important is the accuracy of the initial conditions. In November 1984, a fine mesh data assimilation scheme was implemented operationally in order to improve the analyses of smaller scale features. Many of the features which influence our weather are relatively small and it is particularly important for short range prediction that these small scale features are resolved accurately by the analysis. Prior to the implementation of the finemesh data assimilation scheme, the starting point for the fine mesh forecast was an interpolation from a coarser global data assimilation field.

The quality of the analysis is largely determined by the availability of data and the quality of that data. Much of our weather comes from the west and the data coverage over the North Atlantic ocean is often insufficient to define small scale features precisely. Satellite data has long been used to supplement the conventional surface based observing network and has proved of great benefit in data sparse areas. Until recently the only source of satellite temperature sounding data was the SATEM messages sent from Washington on the Global Telecommunications System. This data has a resolution of 300 Km and a spacing of some 600 Km which is quite unsuitable for defining the small scale sub-synoptic system. Locally retrieved sounding data has recently become available on a much higher resolution via the HERMES system and we are now able to assess the impact of such data on operational analyses and forecasts.

2. The Data

The system for retrieving and processing local area sounding data, known within the Meteorological Office by the acronym HERMES has been described by Eyre and Jerrett (1982). The aims of the system were, firstly, to provide satellite sounding data rather more rapidly than was previously available by eliminating the processing and transmission delays. Secondly the system was designed to exploit to the maximum the potential resolution of the High-resolution Infra-Red Radiation Sounder (HIRS). The result is that we have satellite temperature data available on an 80 km resolution within a roughly circular region of about 2500 km radius of the receiving station at Lasham, and with the minimum of delay.

The data has been available to the Central Forecast Office from mid 1983 and it has been used in the coarse mesh data assimilation system at a degraded resolution equivalent to that of SATEMS since September 1984. We are now in a position to objectively analyse data from the HERMES system at its full resolution using the fine mesh data assimilation scheme. The case chosen for investigation dates back to 9 February 1984. Both US polar orbiting satellites NOAA-7 and NOAA-8 were providing data at that time, so there were frequent passes over the local area. Data from passes at 0220 Z, 0400 Z, 0540 Z, 0630 Z, 0810 Z and 1210 Z were used. For these six passes, the satellite crosses the 50°N latitude at 25°E, 5°W, 25°W, 20°E, 0°E, 40°E respectively. Some 600 observations are available from each pass, with the exception of the last pass which is on the extreme eastern boundary of the fine mesh model area. Table 1 gives an indication of the volume of data available from the HERMES system relative to that from other observing systems. The numbers refer to the data actually used during the fine mesh data assimilation period. The 12 hour period has been split into four three hour periods for reasons which will become clear in the following section. For surface and radiosonde data the numbers refer to those reports valid at 3 Z, 6 Z, 9 Z and 12 Z. For aircraft and satellite data the numbers refer to observations within $1^1/_2$ hours of the analysis times.

Only small numbers of surface land data are used at 3 Z because during the early stages of the fine mesh data assimilation period an adjustment to a finer mesh topography takes place which precludes the use of surface pressure data. The absence of aircraft and satellite cloud track wind data at 12 Z reflects a processing problem on this particular day. Normally one

might expect up to 200 wind observations from AIREPS and SATOBS at that time. The SATEMS were not used in this study, the number given is that which would have been used operationally (none over high land)

	3Z	6Z	9Z	12Z
RADIOSONDE	0	102	3	123
SYNOP	37	523	916	512
SHIP	56	212	94	170
DRIBU	10	6	9	7
(SATEMS)	17	23	28	19
HERMES	1399	1152	676	365
AIREP	124	128	45	-
SATOB	0	0	11	-

Table 1 Number of Observations available.

3. The fine mesh data assimilation scheme

In order to make clear how the observations are used, we will give a brief description of the fine mesh data assimilation scheme. The starting point for the fine mesh data assimilation cycle is an interpolated coarse mesh analysis which verifies at T-12 hours, that is 12 hours prior to the forecast start time. This is a simple bi-linear interpolation to the latitude-longitude fine mesh grid, which has twice the resolution of the coarse mesh model and has the same 15 levels and the same terrain following vertical coordinate system. The fine mesh model grid covers an area enclosed by longitude lines 80°W and 40°E and by latitude lines 80°N and 30°N. The dimensions of the grid are 129 points E-W and 67 points N-S giving an approximate resolution of 75 kms. Lateral boundary values are required to allow for the movement of synoptic features through the edges

of the forecast region. The boundary tendencies for the prognostic variables are derived from a coarse mesh forecast starting from the same coarse mesh analysis at T-12 which was used to provide the interpolated fine mesh field. These tendencies are applied through the data assimilation cycle as well as the subsequent forecast.

The data assimilation cycle consists of four separate 3 hour assimilation periods as illustrated in Figure 1. The observation used in each period are those which are valid at T-9, T-6, T-3 and T+0 hours respectively, although an observation time window of $\pm 1^1/_2$ hours allows all observations which fall within that 3 hour window to be used and they are assumed to be valid at the analysis times. The method used to quality control, select, weight and assimilate the data is analogous to that used in the global coarse mesh data assimilation scheme (Bell, 1983). Each of the assimilation periods is composed of the following sequence of steps. The first step involves conversion of variables from those observed to those being analysed, ordering in latitude bands and generally putting the observations in an appropriate format. For satellite temperature sounding data this implies a conversion to potential temperature.

Following this there are two quality control checks which are designed to be complementary. The first check involves raising a flag on every observation which departs substantially from the first guess, which is a forecast verifying at the observation time.

$$(\psi_{OB} - \psi_{FG})^2 \geq N^2(\epsilon_{OB}^2 + \epsilon_{FG}^2) \qquad 3.1$$

The observations (ψ_{OB}) are suspect if the inequality in equation 3.1 is satisfied. Where ψ_{FG} is the first guess value at the observation point and ϵ_{OB}, ϵ_{FG} are assumed errors for observation and first guess respectively.

These suspect observations are not allowed to quality control other observations in the second check but they may be reinstated if their departure from the expected analysis using neighbouring observations does not exceed a predetermined level. The statistical interpolation method used to analyse the data involves the calculation of a correction to the first guess. The correction is expressed as a weighted average of the departures of observed values from the first guess, the weights themselves being selected so that the statistically expected errors in the analysis are minimised. The weights are a function of observational error, first guess error and the correlation of errors between neighbouring points. The prescribed observation errors are in the range 2°C-$2\frac{1}{2}$°C for satellite temperatures. For comparison, radiosonde temperatures are assumed to have errors slightly over 1°C at low levels and increasing with height such that the assumed errors become greater than those for satellite temperatures above 150 mb. These values are based on a study of observation errors from FGGE data, with minor revisions since then to reflect improvements to the satellite observing system. In general higher observation error implies lower weight.

A second statistical interpolation analysis is performed using all the unflagged data to select the data and calculate the required weights for determining corrections appropriate to the analysis grid. The selection

involves firstly a preselection of the nearest 30 observations within a cylinder of influence around the point. Some care is taken to avoid one observation type swamping other types by limiting the number of a given type which are selected. This limitation is particularly necessary when one considers the high density of observations from the HERMES system relative to that of other observation types. In the second selection stage the seven best pieces of data are selected, the best being those which when taken singly reduce the expected analysis error by the greatest amount.

The corrections calculated by this method are assimilated directly into the fine mesh forecast model using a repeated insertion technique. At each model timestep ($7^1/_2$ minutes), during a three hour period, a small fraction ($\Delta\psi$) of the weighted average of the difference between the forecast (ψ_m)and the observed values (ψ_i) is added into the model.

$$\Delta\psi = \lambda\Sigma W_i \, (\psi_i - \psi_m) \qquad 3.2$$

In this way the model adjusts slowly towards the observed state without generating spurious large non-meteorological motions. Wind increments which are geostrophically in balance with the observed mass field increments are also used to correct the model wind field, in addition to any corrections based on observations of the wind field. This is particularly useful in assisting the model to adjust towards satellite temperature data which is unsupported by wind observations.

4. Results from the HERMES case study, 9 February 1984

In order to access the impact of the full resolution satellite temperature data, we decided to compare two parallel assimilations closely at each of the four stages of the fine mesh assimilation cycle. The first of these assimilations, which we will call the 'Control run', used all available surface and radiosonde observations, but no satellite information at all. The second assimilation, to be called the "HERMES run', used all available surface and upper air information, including full resolution satellite soundings produced by the HERMES system.

The starting point for our investigation was the coarse mesh analysis for 00 GMT, 9 February. The main synoptic features at this time are shown in figure 2. So far as the British Isles was concerned, the dominant feature was the large anticyclone, centred to the west of Spain. During the twelve hour period of the fine mesh assimilation cycle, this anticyclone drifted slowly northwards, with a ridge extending northeastwards over most of England and Wales. The warm front approaching Western Scotland and Ireland was a weak feature south of 60 degrees north.

4.1 Impact on the 1000-500 mb thickness

First, a three hour fine mesh forecast was run from DT. 00 GMT, 9th February, to generate the first-guess field for 03 GMT. This was used to quality control all observations received between 0130 and 0430 GMT. Observations which passed the quality control checks were then assimilated into a three-hour forecast from 00 GMT, as described in the previous

section.. The satellite information used in the 'HERMES' assimilation was obtained from two passes at 0220 and 0400 GMT. The observations from these two passes, which crossed latitude 50 degrees north at 25 degrees east and 5 degrees west respectively, merged to give an almost continuous coverage of satellite temperature information over the fine mesh area, east of 15 degrees west.

Table 1 gives the details of the observations used in the 03 GMT assimilation stage. The table shows that very little data was used in the 'Control' assimilation, and in consequence, the 03 GMT thickness analysis (shown in figure 3) was almost identical to the background field. In contrast, the 'HERMES' assimilation used 1399 extra temperature observations from the satellite soundings. The main feature of interest in figure 3 was the position and depth of the thermal trough over Europe, marked by the 522 dm thickness line. In this region, the thickness values derived from the satellite soundings, were at about 5 dm lower than corresponding values in the Control analysis. The impact of these lower values on the analysis becomes apparent when the 'HERMES' thickness analysis for 03 GMT is compared with the 'Control' analysis. In the 'HERMES' analyses, there has been a marked decrease in thickness values on and east of the thermal trough axis. On the western side of the trough, over the North Sea and France, thickness values have been raised slightly. Figure 4 shows the thickness differences between the 03 GMT analyses [Hermes minus Control].

After the completion of the 03 GMT assimilation, a three-hour fine mesh forecast was run to generate the first guess field for 06 GMT. This was followed by the assimilation of observations received during the period 0430 to 0730 GMT. Table 1 shows that many more observations were used in the 06 GMT assimilation stage in comparison with the 03 GMT stage. However, most of the radiosonde data consisted of wind information only,with only a few temperature soundings. In addition, the 'HERMES' assimilation used 1152 temperature observations from satellite soundings. These temperatures were obtained from two passes at 0540 and 0630 GMT, which crossed latitude 50 degrees north at 25 degrees west and 20 degrees east respectively. The detailed coverage, together with the derived thickness and thermal winds, is shown in figure 5. Of particular interest are the low thickness values over the continent.

Figure 6 shows the 06 GMT thickness analysis from the 'Control' assimilation. The impact of satellite observations on the 'HERMES' assimilation can be seen by studying figure 7. This shows the thickness differences between the two 06 GMT analyses [HERMES minus Control]. Negative values have been shaded, showing that in these areas, the assimilation of satellite temperatures has reduced the thickness. There are two main areas in which the use of satellite temperatures has reduced the thickness substantially.

The first area is in the region of the thermal trough over Europe, in which the thickness has been lowered by a maximum of 8 dm over Northern Italy and the Adriatic. The 516, 522 dm thickness lines are both about 5 degrees further south in the HERMES analysis. If we compare the HERMES thicknesses with the radiosonde values at 00 and 12 GMT, the HERMES values look too low, indicating a cold bias in the HERMES data below 500 mb.

The second area in which the use of temperatures from satellite soundings has caused a reduction in thickness values is the area between 35 and 50 degrees west. This is an important area of the analysis, since it contains a depression (centred at 48 N, 46 W at 06 GMT), which was deepening and moving northwards, with the associated cold front moving slowly eastwards. The features are in a data-sparse region over the Atlantic, and it is in this kind of situation that we need accurate satellite information to improve the analysis. Unfortunately, we do not have enough information in this area to judge whether the lowering of thickness values by the use of satellite data was correct.

Comparing figures 5 and 7, we notice that some of the largest differences occur at 40 to 50 degrees west, which lies just to the west of the HERMES swath in the 0540 GMT satellite pass. The radius of influence of a satellite observation extends at least 5 degrees. This implies that some of the largest differences in thickness values between the 'HERMES' and 'Control' runs were due to satellite observations at the edge of the swath. These observations may have been subject to larger errors due to the oblique angle of view.

After the 06 GMT analysis was completed, a three-hour fine mesh forecast was run to generate the first guess field for 09 GMT. Table 1 gives the details of the observations used in the 09 GMT assimilation. This time only one satellite pass at 0810 GMT was used. This pass crossed latitude 50 degrees north at the meridian, producing extra temperature data for the 'HERMES' assimilation over a strip of the fine mesh area between 15 degrees west and 15 degrees east.

Figure 8 shows the 09 GMT thickness analysis from the 'Control' assimilation, whilst figure 9 shows the differences between the 'Control'and 'HERMES' thickness values. Again, the negative shaded areas mean that the HERMES thickness is less than the corresponding 'Control' values. The differences in figure 8 show the accumulative effect of using satellite observations at 03, 06 and 09 GMT. Over most of the chart the differences are negative, suggesting an overall cold bias in HERMES data below 500 mb. The maximum differences occur in the thermal trough over the continent, which has been broadened and deepened in the 'HERMES' assimilation. The differences in the thickness values between 30 and 40 degrees west have remained in the analysis from 06 GMT.

For the final stage of the assimilation a three hour fine mesh forecast was run from 09 GMT to generate the 12 GMT first guess field. The satellite pass at 1210 GMT crossed latitude 50 degrees north at40 degrees west, providing observations only over Scandinavia and Eastern Europe. It was more interesting, therefore to assess the effect of the 12 GMT radisonde data, especially over land in Western Europe. By the cut-off time 1330 GMT, many full temperature soundings in this area had been

received and used in the assimilation. Whereas, as table 1 shows, comparatively few HERMES observations were used in the 12 GMT assimilation, and these were over Scandinavia and Eastern Europe.

Figure 11 shows the differences remaining in the thickness analysis at 12 GMT between the 'HERMES' and 'Control' assimilations. Most of the differences over Western Europe and the Mediterranean have been reduced or removed altogether. Some larger differences still remain over Eastern Europe. From this area and also from data-sparse regions in the Atlantic, radiosonde data was received too late to be used in the 12 GMT assimilation. To confirm the correcting effect of the 12 GMT radiosonde data, a 'special HERMES' assimilation was run, using all satellite data but excluding all radiosonde data. Figure 12 shows the resulting differences in thickness values at 12 GMT between the 'Control' analysis and the 'No radiosonde HERMES' analysis. The differences are much larger and mainly negative, confirming both the correcting influence of 12 GMT radiosonde data over land and also the cold bias of satellite soundings below 500 mb.

4.2 Impact on the upper troposphere

During the assimilation period, the tropopause remained low over the continent (below 300 mb) in the vicinity of the upper trough, and high over Western Europe and the Eastern Atlantic, (above 200 mb), in association with the upper ridge. Two jet streams were of importance;

a. a northerly jet stream from Western Norway to Sardinia,

b. a southwesterly jet stream between Greenland and Iceland.

We studied in detail charts at 300, 250 and 200 mb from both the 'HERMES' and the 'Control' assimilations, in order to assess the effect of temperatures from satellite soundings on the upper troposphere. The temperature charts at 03, 06, 09 GMT showed significant differences. Over most of the charts, the effect of using temperatures from satellite soundings had been to raise the temperature, locally by as much as 6 to8°C. This warming effect was most noticeable at 200 mb, and we have included the chart at figure 13 as an example. Figure 13 shows the 200mb temperature differences [HERMES minus Control] at 0600 GMT, resulting from the assimilation of HERMES data from the four satellite passes at 0220, 0400, 0540 and 0630 GMT respectively. The differences are mostly positive, implying a warm bias in satellite temperatures in the region of the tropopause. The highest increases in temperature are observed at 10 to 15 degrees, west, in the region of the upper high, and also at 30-40 degrees west, which coincides with the edge of the satellite swath at 0540 GMT.

However, when we compare the temperature charts at 12 GMT, (figure 14) it is surprising to notice that most of the differences over Western Europe and the Mediterranean have almost disappeared. We think that this is due to the powerful correcting influence of 12 GMT temperatures from radiosonde ascents. Some large differences remain, but these are over Eastern Europe and the Atlantic, and from these regions no radiosonde data has been received. Figure 15 confirms this statement. This chart shows the

temperature differences at 200 mb between the 'No radiosonde HERMES' analysis and the 'Control analysis'. Note, in particular, the contrast between figures 14 and 15 over Western Europe and the Mediterranean.

The warm bias of HERMES data in the region of the tropopause is also seen by comparing the tephigrams in figure 17. Figure 17a shows the difference in the 12 GMT temperature profiles between the Hemsby radiosonde ascent and the background field, for the 'Control' assimilation. Figure 17b shows the corresponding profiles for the 'HERMES' assimilation. The 'HERMES' background still contains the influence of temperatures from satellite soundings at 03, 06 and 09 GMT, and is 3°C warmer at 250 and 200 mb than the 'Control' background.

We were concerned that the large differences in temperature and geopotential heights observed in the first three stages of the assimilation may have affected the strength of the jetstreams. Table 2 shows the differences in the strength of the jet cores of the two jet streams. The maximum difference is noticed in the southwesterly jetstream between Iceland and Greenland, where the maximum wind has been reduced by 19 to 23 kt in the 'HERMES' analysis between 06 and 12 GMT. The northerly jet stream over the North Sea and Europe is less affected, presumably due to the much wider coverage of upper air stations

JET	ASSIM.	03Z	06Z	09Z	12Z
Southwesterly Jetstream between) Iceland and Greenland.)	CONTROL	159	173	184	169
	HERMES	167	154	161	150
Northerly Jetstream between) West Norway and Sardinia)	CONTROL	169	174	161	157
	HERMES	170	178	167	150

Table 2 Strength of Max. Wind

4.3 Impact near the surface

In this case study, temperatures from satellite soundings were generally too cold at low levels, especially below 900 mb. This is shown by studying figure 17, where we are comparing the model first guess temperature profile at 12 GMT with the collocated radiosonde ascent at Hemsby. The 12 GMT first guess field is a three-hour forecast from 09 GMT and contains no 12 GMT data. By comparing the first guess profiles in figures 17a and 17b, we can see that the 'HERMES' profile is 2 to 3 degrees colder below 850 mb. This coldness at low levels of HERMES data is confirmed by figure 16, which shows the difference in the 06 GMT 1000 mb temperatures [HERMES minus Control].

The cold bias at low levels is caused mainly by inaccuracies in the radiance data due to cloud contamination. If cloud is present, then, during the processing of the data, the radiance which would have been measured in the absence of cloud, is calculated from HIRS radiances in adjacent fields of view. With large areas of thick cloud, this method cannot be used, and so these radiances are discarded and gaps appear in the

retrieval fields. These gaps may be partly filled by using microwave data. These facts may explain partly the large temperature difference of 9°C in the Mediterranean between Sardinia and Italy. At 06 GMT, a depression was moving southeastwards over Italy, and the thick cloud associated with this depression means that the radiance data in this region was inaccurate due to cloud contamination. Also, the fact that the thermal trough over Europe was deepened and moved southeastwards in the 'HERMES run' means that the cold front associated with the depression was also moved southeastwards, allowing the penetration of colder air into the Mediterranean.

5. Discussion

The above study has indicated several problem areas which deserve further attention. Regarding the HERMES data we have highlighted three problem areas concerning biases in that data. The problems at the edge of the swath have been discussed in the preceding section. The satellite meteorology branch have examined co-location statistics of HERMES data differences from radiosondes for various positions along the satellite swath. (Turner, private communication). These statistics agree with our conclusions about the quality of the data towards the edge of the swath and suggest that the empirical correction to correct for the differing viewing angle is not always appropriate. In view of this evidence it was decided to eliminate three observations on each side of the swath.

The cold bias at low levels which is illustrated by figure 16, the 1000 mb temperature differences between the control run and the HERMES run, is also worrying. These biases persist into a forecast as can be seen from the tephigrams displayed in figure 17. The extent of the problem can be seen in figure 18, where the differences of the 3 Z HERMES observations

from the models first guess are displayed for three levels. The plots are in terms of a histogram giving the percentage of observations as a function of the temperature difference. The mean difference for the lower troposphere layer is -3°C and around 25% of observations are in excess of 6°C cold (dashed line). The observations are much better behaved in the mid-tropospoheric layer (solid line). Obviously such biases are quite unacceptable and the simple option to exclude 1000 mb temperature observations from the analysis has been taken. Figure 18 also highlights the third problem area which was disucssed in the previous section, namely the warm bias at the tropopause level (dot-dash line). The histogram of observed differences in the 200-150 mb levels is clearly bimodal with peaks at +1°C and +9°C. The small warm bias of the majority of observations can be explained by the coarseness of the vertical resolution of the sounder. However the problems of the 25% of observations which differ by more than 6°C from the model are not so easily explained.

Adams (1984) has suggested that the observations are unable to portray conditions which deviate substantially from the climatological case. In this case the tropopause is higher than normal to the west of the Greenwich Meridian and the largest 200 mb temperature differences are in this area (figure 12). Another possible cause is contamination of the radiances by cloud. It is not appropriate to reject all data at tropopause levels since there is clearly some merit in the majority of observations. The analysis procedures must be tuned to make the best use of the data that is available although clearly further work is required to improve the data to the extent that the biases discussed above are eliminated.

	CONTROL	HERMES	HERMES 1	HERMES 2
3z	25.4	4.4	25.4	25.4
6z	10.6	3.3	7.8	9.4
9z	19.2	2.0	8.2	12.7
12z	2.0	1.5	1.1	0.7

TABLE 3

% of HERMES rejected (above 700 mb)

'HERMES' is original HERMES assimilation run.
'HERMES 1' is repeat HERMES run with stricter quality control.
'HERMES 2' is as HERMES 1 with reduced weight given to HERMES.
'CONTROL' is no HERMES run (The HERMES data were quality controlled as for HERMES 1 but not used).

The first option is to improve quality control procedures to exclude the worst of the poor soundings. Table 3, column 2 gives the percentage of observations rejected by the analysis at each assimilation cycle, in the HERMES RUN. Very few levels are rejected when one considers the large biases that are apparent from figure 18. There seem to be two reasons for this. The problem gets worse in the later cycles which suggest that the model is adjusting towards a 'HERMES climatology' and therefore the observations are accepted more readily. Another reason is that the errors in the HERMES data are highly correlated and the second stage of the qualtiy control procedure, whereby observations are compared against their neighbours, unflags many of the observations which had failed the check against the model first guess.

Much of the above discussion has concentrated on the difference between the control run and the HERMES run. The conclusions which have been drawn are based on an assumption that the control run is substantially unbiased and that the differences suggest biases in the HERMES data. A

simple test of the quality of an analysis is to see how well a short forecast from that analysis verifies against a set of good quality observations.

		CONTROL	HERMES	HERMES 1	HERMES 2
below 700 mb	mean	0.75	2.05	1.22	0.93
	rms	1.87	2.64	2.04	1.86
200-700 mb	mean	-0.73	-1.81	-1.56	-1.18
	rms	2.45	3.55	3.24	2.69
above 200 mb	mean	0.49	-0.05	0.09	0.36
	rms	4.13	4.63	4.72	4.37

TABLE 4a

Fit of first guess temperature field to radiosonde data at 6Z
Runs as defined in Table 3
Mean = (observation - first guess)

		CONTROL	HERMES	HERMES 1	HERMES 2
below 700 mb	mean	0.75	1.68	0.87	0.85
	rms	1.85	2.73	2.25	1.98
200-700 mb	mean	-0.01	-0.75	-0.72	-0.45
	rms	2.46	3.34	3.27	2.83
above 200 mb	mean	0.46	-1.28	-0.93	-0.27
	rms	6.55	6.95	7.08	6.68

TABLE 4b

as for Table 4a but for 12z data

Table 4a gives the mean and rms fit of the 3 hour forecast from the 3 Z analysis against 6 Z radiosonde data for three layers. Column 1 gives details of the Control run and column 2 gives details of the HERMES run. Columns 1 and 2 of Table 4b give the same information regarding the fit of the 3 hour forecast from the 9 Z analysis to verifying 12 Z radiosonde data. In nearly all cases the mean and rms errors are worse in the HERMES run than they are in the Control run, implying that the additional information is not adding anything useful to the analyses, at least over the radiosonde network.

6. Further Experiments

Given all the problems with the data and with the way it was analysed, it was decided to repeat the HERMES run with modifications to avoid using some of the suspect data. This repeat run (HERMES 1) with stricter quality control contained the following features

a. No edge of swath data from HERMES

b. No 1000 mb level data from HERMES

c. HERMES data not allowed to quality control other HERMES data

d. Reject a complete sounding if more than 2 levels were flagged

The fourth measure was included because the individual levels cannot be regarded as independent. If several levels are flagged then there is probably a problem with the retrieval, such as cloud contamination or inappropriate regression statistics, which means that other levels should be regarded with suspicion.

The impact of the third and fourth measures can be seen by comparing the flagging details of this run (Table 3, column 3) with the original HERMES run. These figures exclude the edge of swath data and the low level data which were discarded before the analysis stage, but nevertheless substantially more levels are rejected by the analyses quality control procedures. The wide variation in the numbers flagged at different analysis times, reflects the fact that the observations are in different locations. Some air masses (ie those closest to climatology) may be better observed by the HERMES system. Another reason for this is that the ascribed first guess error is allowed to vary spatially and therefore the quality control is stricter in areas such as Western Europe where the first guess error is low.

The quality of the 'HERMES 1' run is best judged by comparing the three hour forecasts from the intermediate analyses (3 Z, 9 Z) against verifying radiosonde data (columns 3 of Table 4a and 4 b). It can be seen that the biases and rms fit are much reduced at lower levels but less so at upper levels compared with the original HERMES run (column 2). However they are still significantly greater than the Control run (column 1).

The implication of this result is that the HERMES data which are allowed to pass the quality control are being given too high a weight. In order to reduce the statistical interpolation weights (W_i in Eqn 3.2) either the observation erors should be greater than presently assumed or the model errors should be reduced. Because quality control decisions would be affected by such a tuning of error levels (see Eqn 3.1), a simpler approach was adopted for the purposes of this case study. The scaling factor λ (Eqn 3.2) for the assimilation increments was halved for HERMES observations in a second repeat of the HERMES run. In this run (HERMES 2), slightly more observations are rejected (Table 3, column 4) indicating that the model is not going as far towards a 'HERMES climatology'. The fit of the three hour forecasts from the intermediate analyses (3 Z, 9 Z) to 6 Z and 12 Z radiosonde data is given in column 4 of Tables 4a and 4 b respectively. There is still evidence of a slight cold bias at low levels and warm bias at higher levels and the rms difference are still slightly higher than in the CONTROL run. The difference in the fit is much more modest than it was in the original HERMES run. This gives us some confidence to expect that if the HERMES data can provide a first guess over the data rich areas which is almost as good as that from the 'Control run' then the first guess and hence analyses over the data sparse Atlantic sector is likely to be improved by the use of HERMES data. The difference fields in Figs 19 and 20 illustrate the impact of HERMES data in this final run. Figure 19 shows the 1000-500 mb thickness difference between the last HERMES run and the CONTROL run at 6 Z and should be compared with Figure 6. The patterns of the two difference fields are very similar but the values in the new run are much more modest. The control assimilation shows that thicknesses over Italy were being analysed as having reduced by up to 6 dm

between 6 Z and 12 Z. We can have reasonable confidence in the 12 Z value which is based on radiosonde data and perhaps might speculate that the cooling was actually occurring a little faster than the Control run suggests to the extent that the HERMES run shows, so the more modest 2-3 dm reduction in 6 Z thickness is entirely feasible.

Figure 19 shows the difference of 200 mb temperature and compares with figure 13. Again the basic pattern of the differences is preserved but the possibly erroneous large positive differences are halved.

7. Conclusions

We have highlighted several inmportant deficiences in data from the HERMES system which seriously limit the usefulness of that data in the context of an objective analysis scheme. The biggest problem is the inaccurate portrayal of the tropopause. Nevertheless with suitable tuning of the analysis scheme along the lines discussed above it is possible to maximise the usefulness of the data and hopefully gain some benefit from this additional data source in the data-sparse North Atlantic.

References

Adams W. 1984 Assessment of HERMES data – a case study comparison with the operational analysis for 2nd March 1984.
Met O 11 Technical Note No 195
(unpublished)

Bell R.S. 1983 The Meteorological office Operational Global Data Assimilation and Forecast System.
6th Conference on N.W.P., June 1983 Omaha Nebraska pp 269–274.
Boston: Amer. Meteor. Soc.

Eyre J.R. and Jerrett D. 1982 Local-Area Atmospheric Sounding from Satellites.
Weather 37 pp 314–322.

Woodroffe A. 1984 Short-range Weather Forecasting – a current assessment.
Weather 39 pp 298–310.

FIGURES

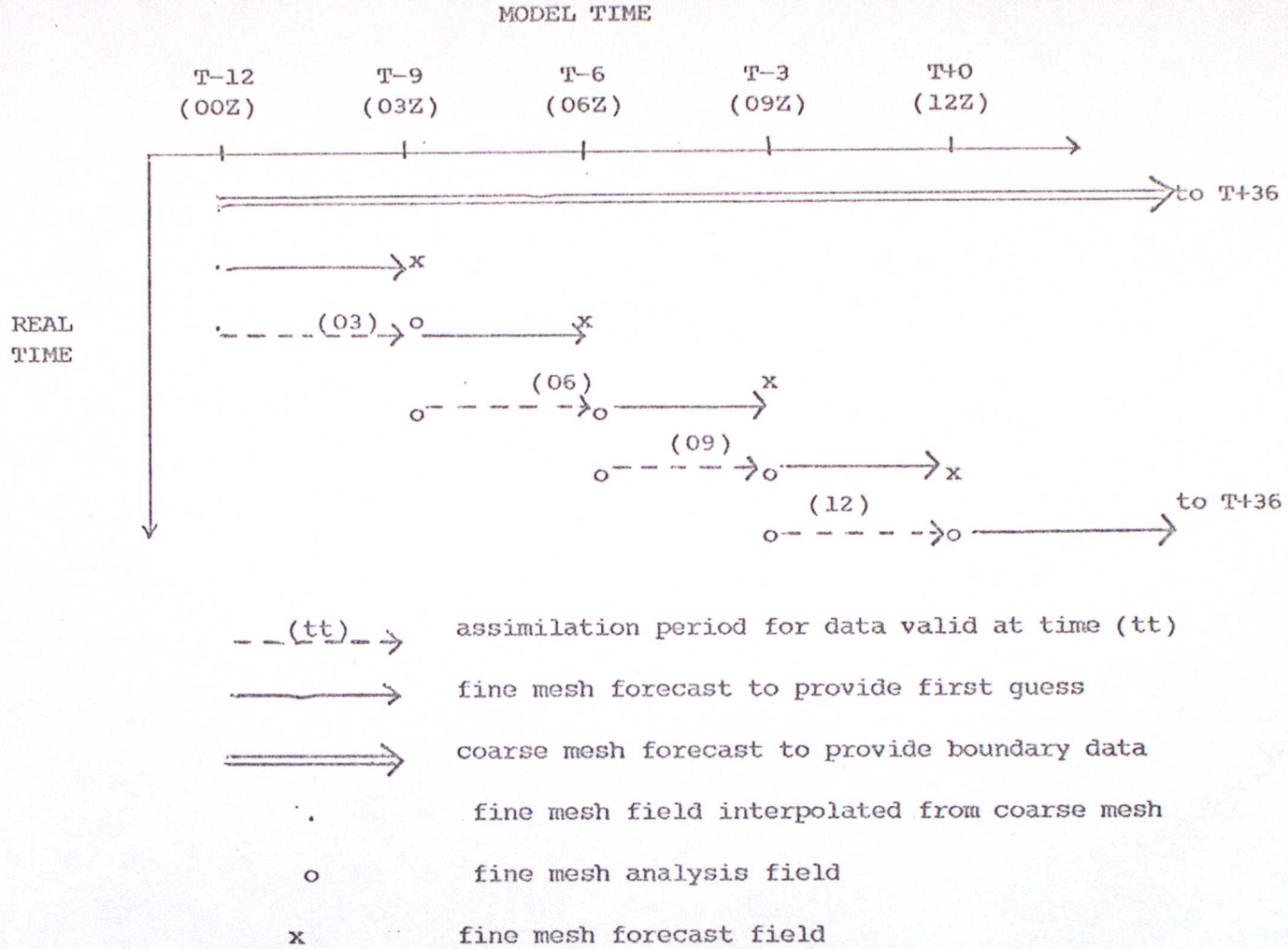

FIG 1

The fine mesh data assimilation scheme

FIG. 2

KS METEOROLOGICAL OFFICE FAX F 28

ASXX EGRR THUR -9 FEB 1984 00 GMT

Polar Stereographic Projection. Standard Parallel 60°N. Original scale 1:20m

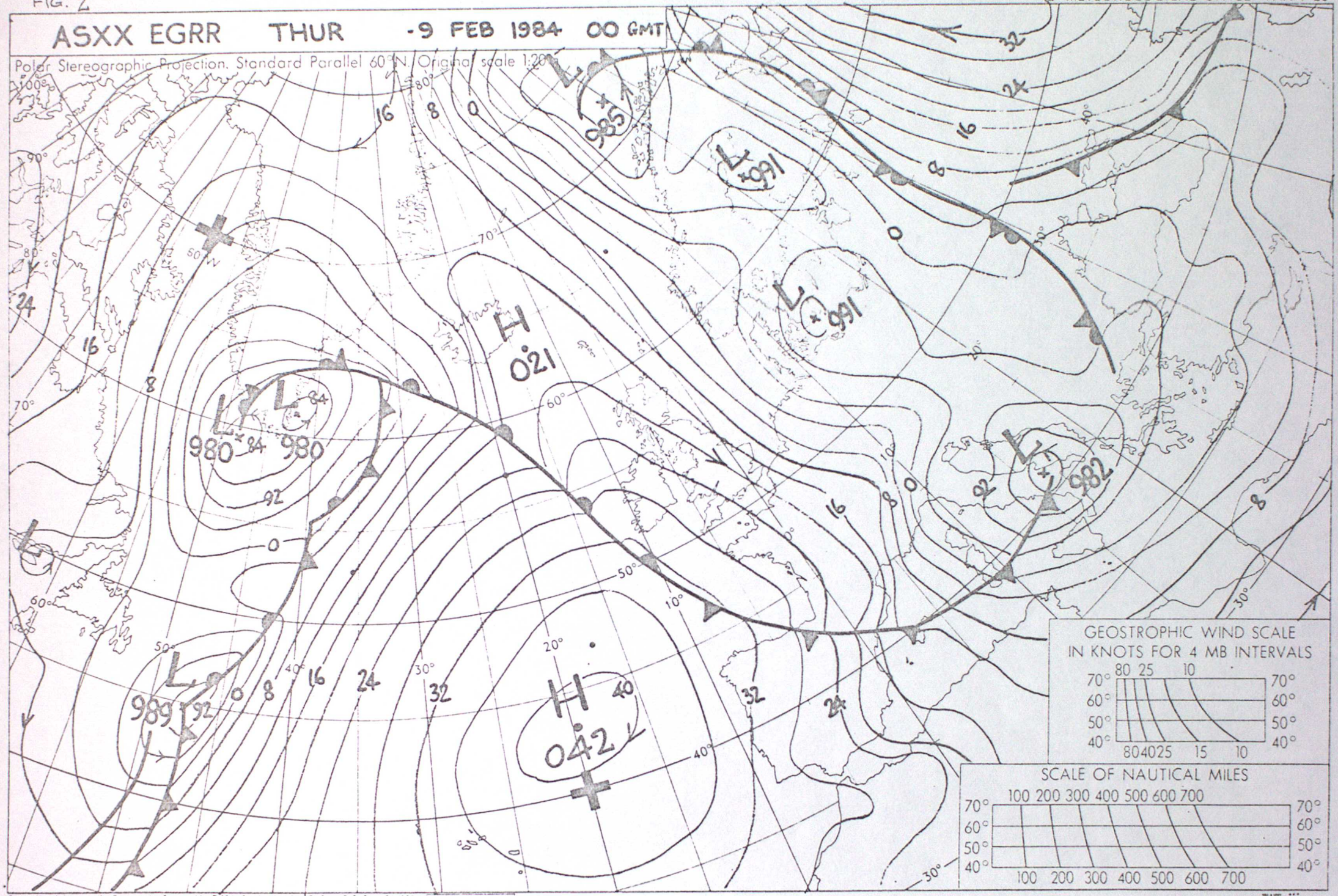

Prepared and drawn in the Cartographic Section, Met.O.18d., Bracknell Met.O. Carto D.O. Form File 269 Amended August 1976

1000-500MB THICKNESS! FINE MESH CONTROL RUN)03Z 9/02/84 FIG. 3
GEOPOTENTIAL HEIGHT
VALID AT 3Z ON 9/2/1984 DAY 40
LEVEL: 500 MB - 1000 MB

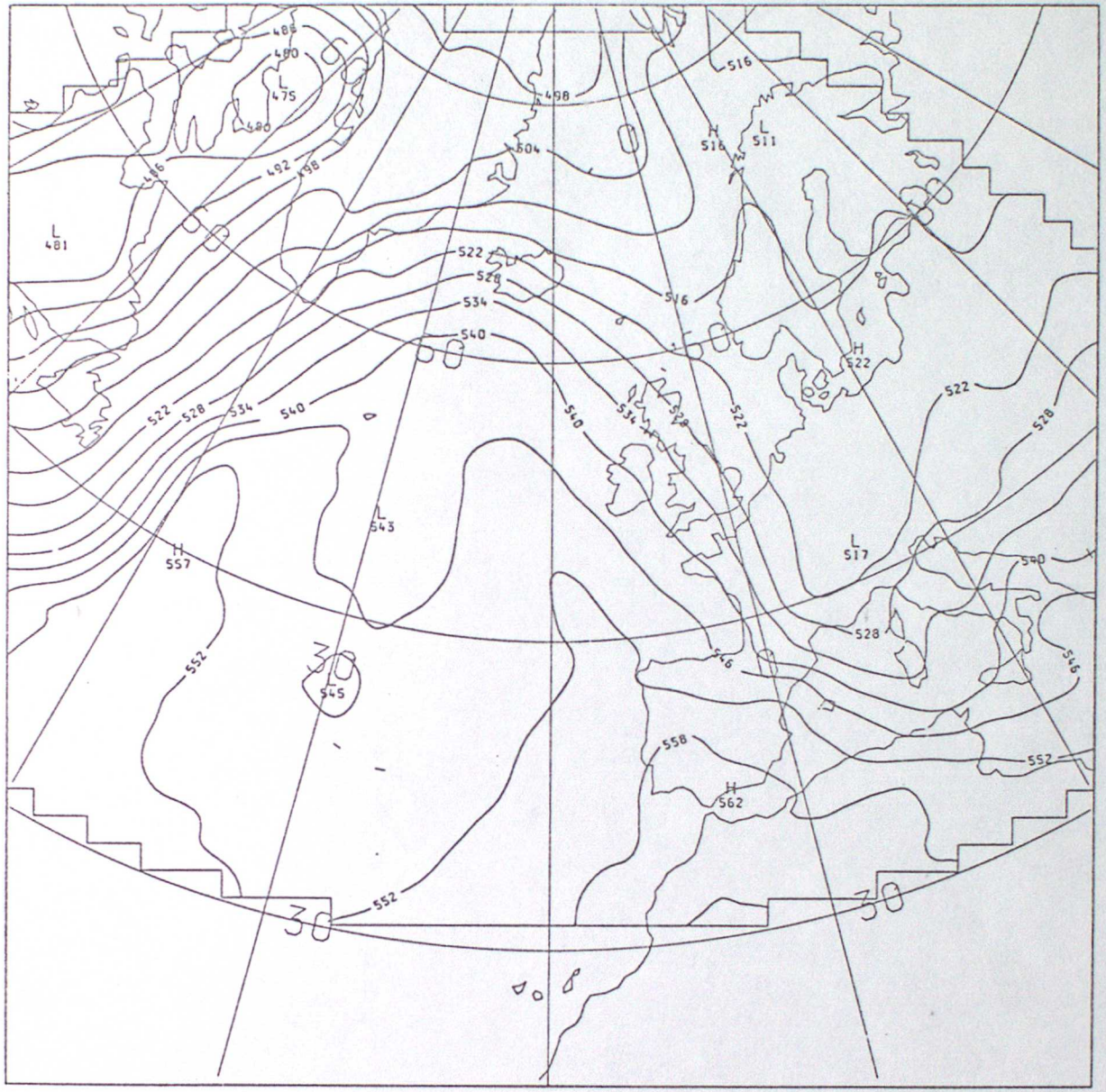

1000-500 THICKNESS(HERMES RUN MINUS CONTROL RUN)03Z FIG. 4
GEOPOTENTIAL HEIGHT
VALID AT 3Z ON 9/2/1984 DAY 40 DATA TIME 3Z ON 9/2/1984 DAY 40
LEVEL: 500 MB - 1000 MB

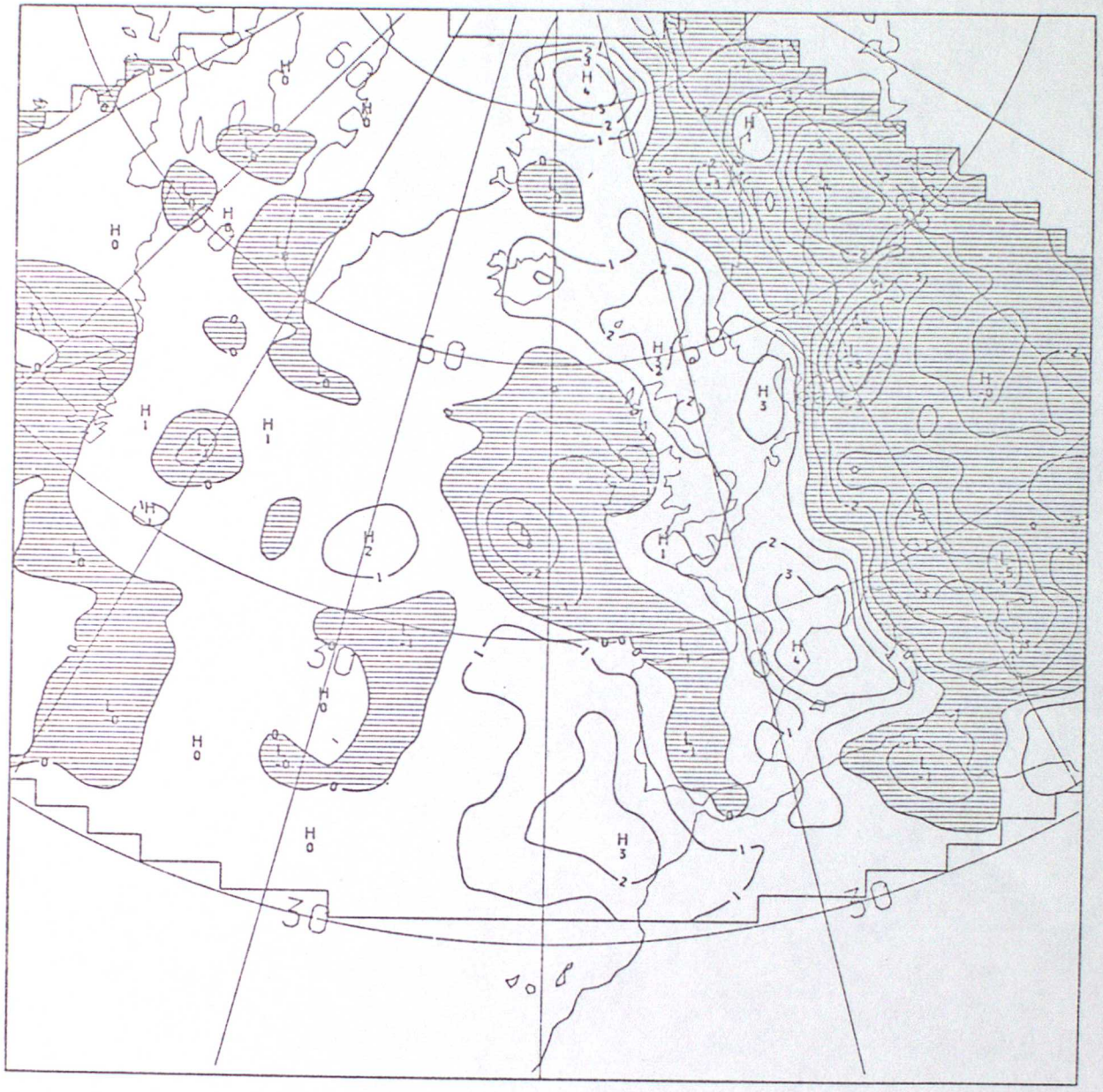

FIG. 5

6Z 9/2/84 HERMES OBSERVATIONS
VERIFYING OBSERVATIONS
VALID AT 6Z ON 9/2/1984 DAY 40
LEVEL: 500 MB - 1000 MB

***M HERMES PLOTTED1040I 61REJ1 MN=-23.3 RMS= 45.6M.1021WIND1 64REJ1 MN= -2.5 RMS= 10.4M/S.

1000-500 THICKNESS(FM ANL WITH NO HERMES DATA)
GEOPOTENTIAL HEIGHT
VALID AT 6Z ON 9/2/1984 DAY 40
LEVEL: 500 MB - 1000 MB

FIG. 6

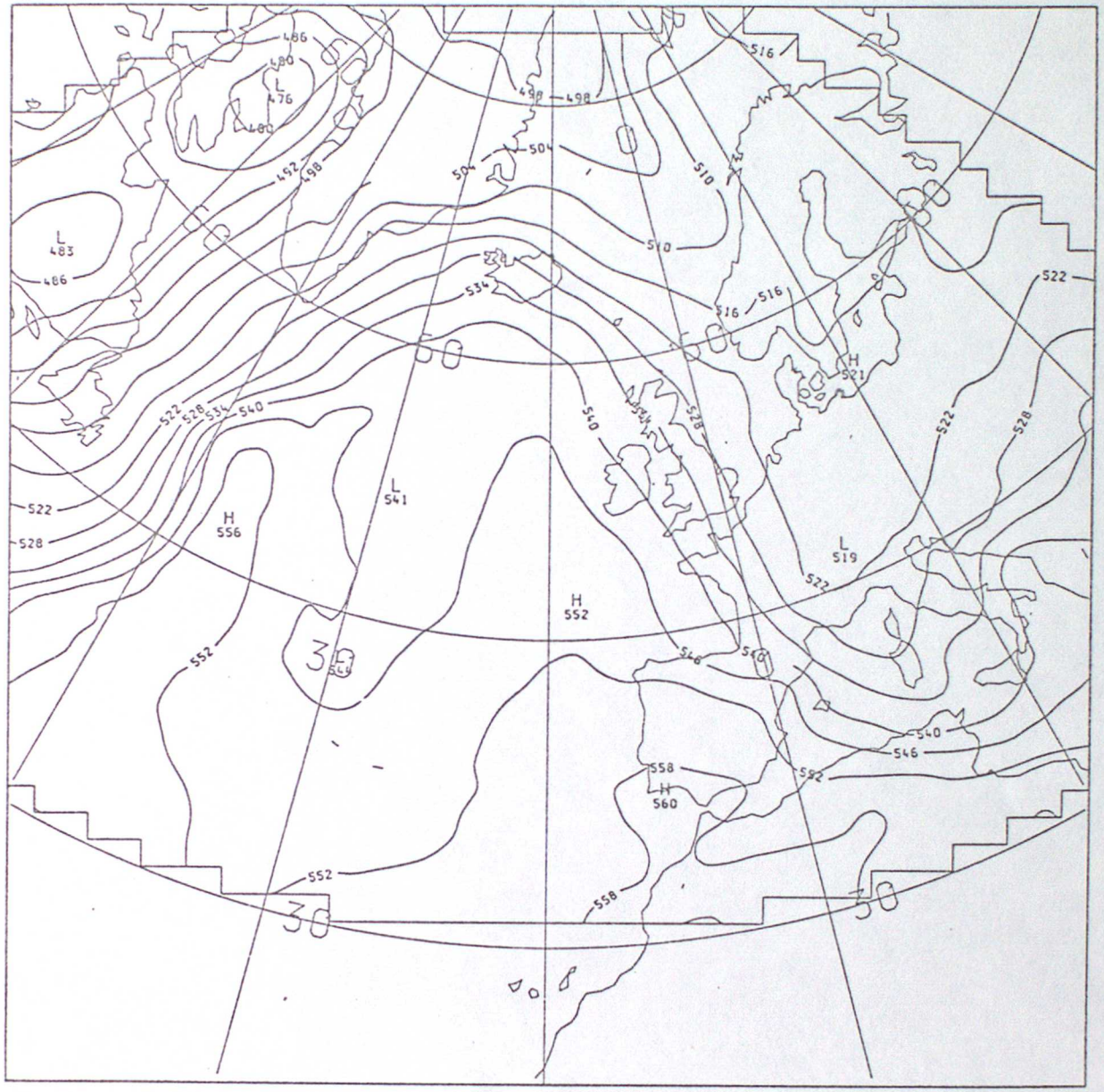

1000-500 THICKNESS(HERMES RUN MINUS CONTROL RUN) FIG. 7
GEOPOTENTIAL HEIGHT
VALID AT 6Z ON 9/2/1984 DAY 40 DATA TIME 6Z ON 9/2/1984 DAY 40
LEVEL: 500 MB - 1000 MB

1000-500 THICKNESS(FM ANL WITH NO HERMES DATA)
GEOPOTENTIAL HEIGHT
VALID AT 9Z ON 9/2/1984 DAY 40
LEVEL: 500 MB - 1000 MB

FIG. 8

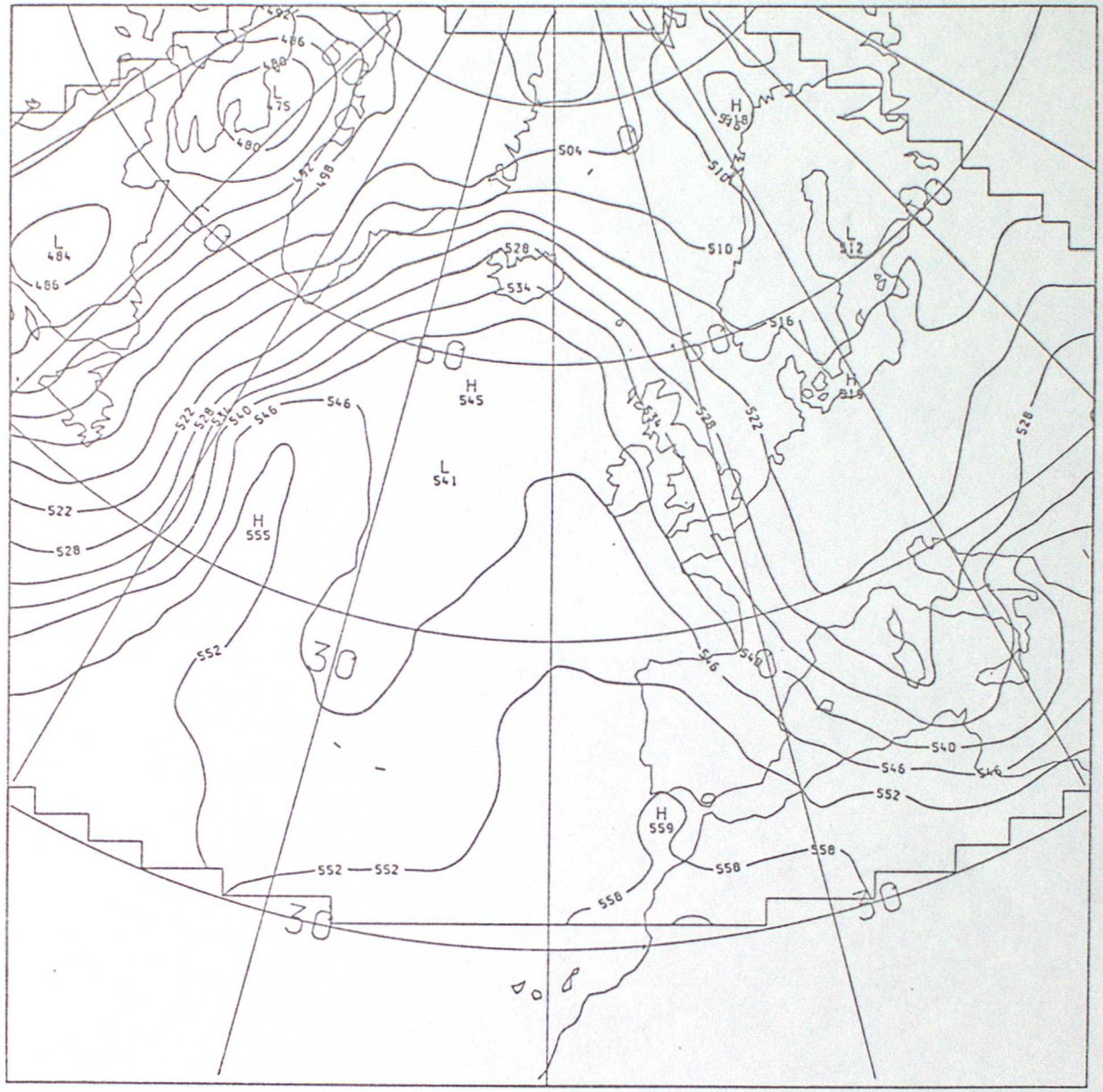

1000-500 THICKNESS(HERMES RUN MINUS CONTROL RUN) FIG. 9
GEOPOTENTIAL HEIGHT
VALID AT 9Z ON 9/2/1984 DAY 40 DATA TIME 9Z ON 9/2/1984 DAY 40
LEVEL: 500 MB - 1000 MB

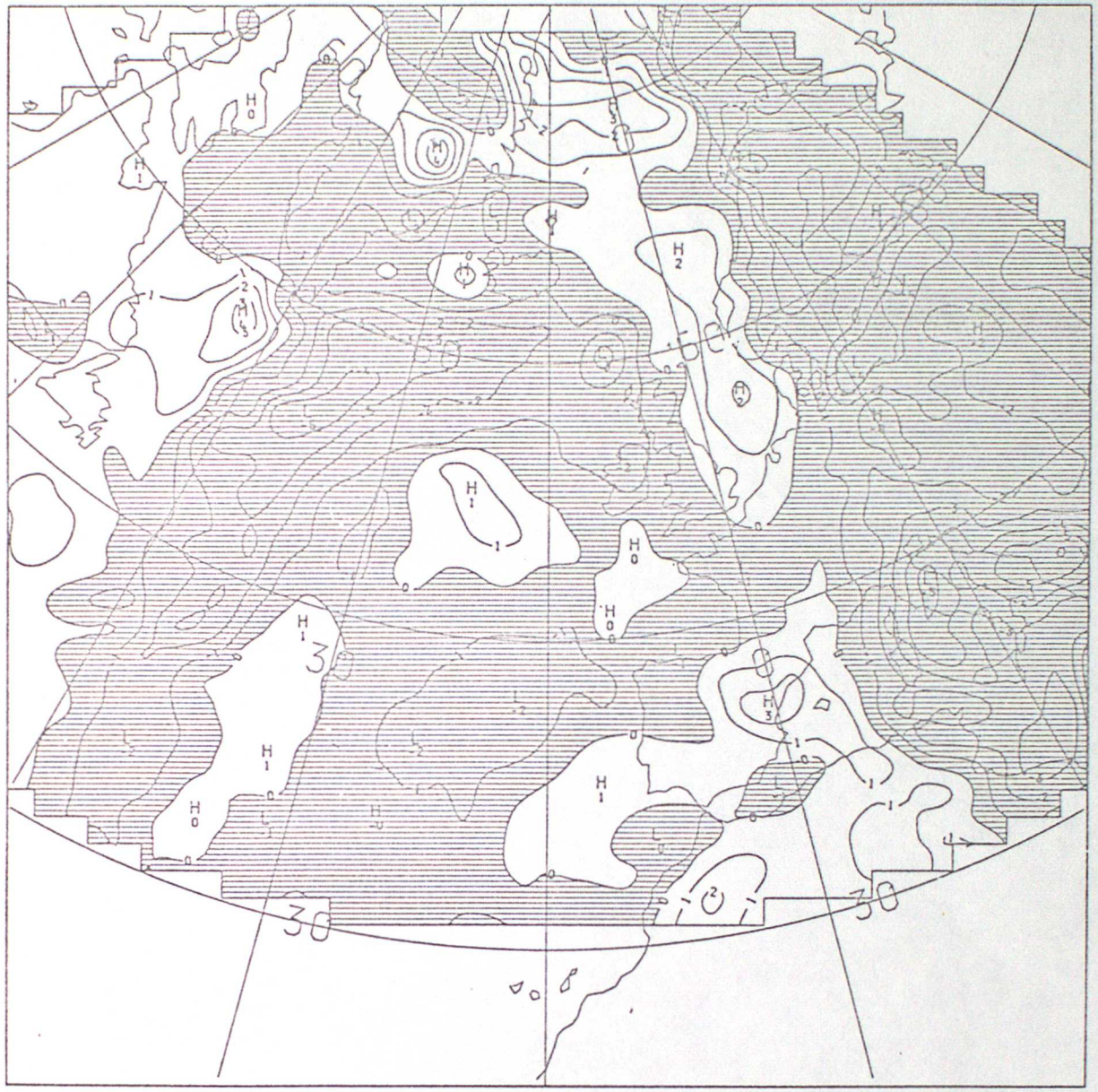

1000-500 THICKNESS(FM ANL WITH NO HERMES DATA)
GEOPOTENTIAL HEIGHT
VALID AT 12Z ON 9/2/1984 DAY 40
LEVEL: 500 MB - 1000 MB

FIG 10

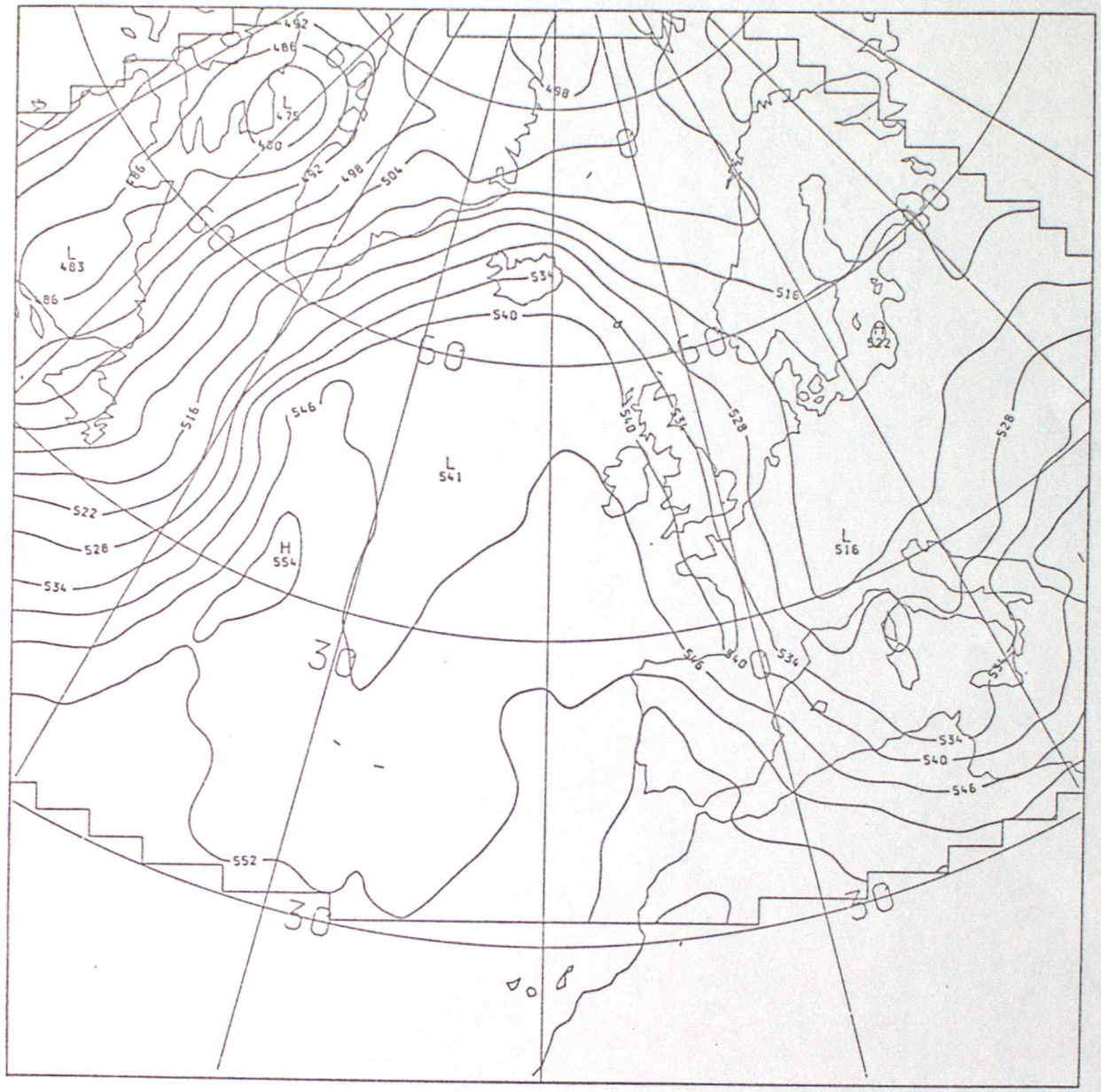

1000-500 THICKNESS(HERMES RUN MINUS CONTROL RUN) FIG. 11
GEOPOTENTIAL HEIGHT
VALID AT 12Z ON 9/2/1984 DAY 40 DATA TIME 12Z ON 9/2/1984 DAY 40
LEVEL: 500 MB - 1000 MB

1000-500 THICKNESS(HERMES(NO RS)RUN MINUS CONTROL RUN) FIG.12
GEOPOTENTIAL HEIGHT
VALID AT 12Z ON 9/2/1984 DAY 40 DATA TIME 12Z ON 9/2/1984 DAY 40
LEVEL: 500 MB - 1000 MB

TEST1-TEST2 F.M ASSIM(HERMES MINUS CONTROL)06Z 09FEB

FIG. 13

TEMPERATURE

VALID AT 6Z ON 9/2/1984 DAY 40 DATA TIME 6Z ON 9/2/1984 DAY 40

LEVEL: 200 MB

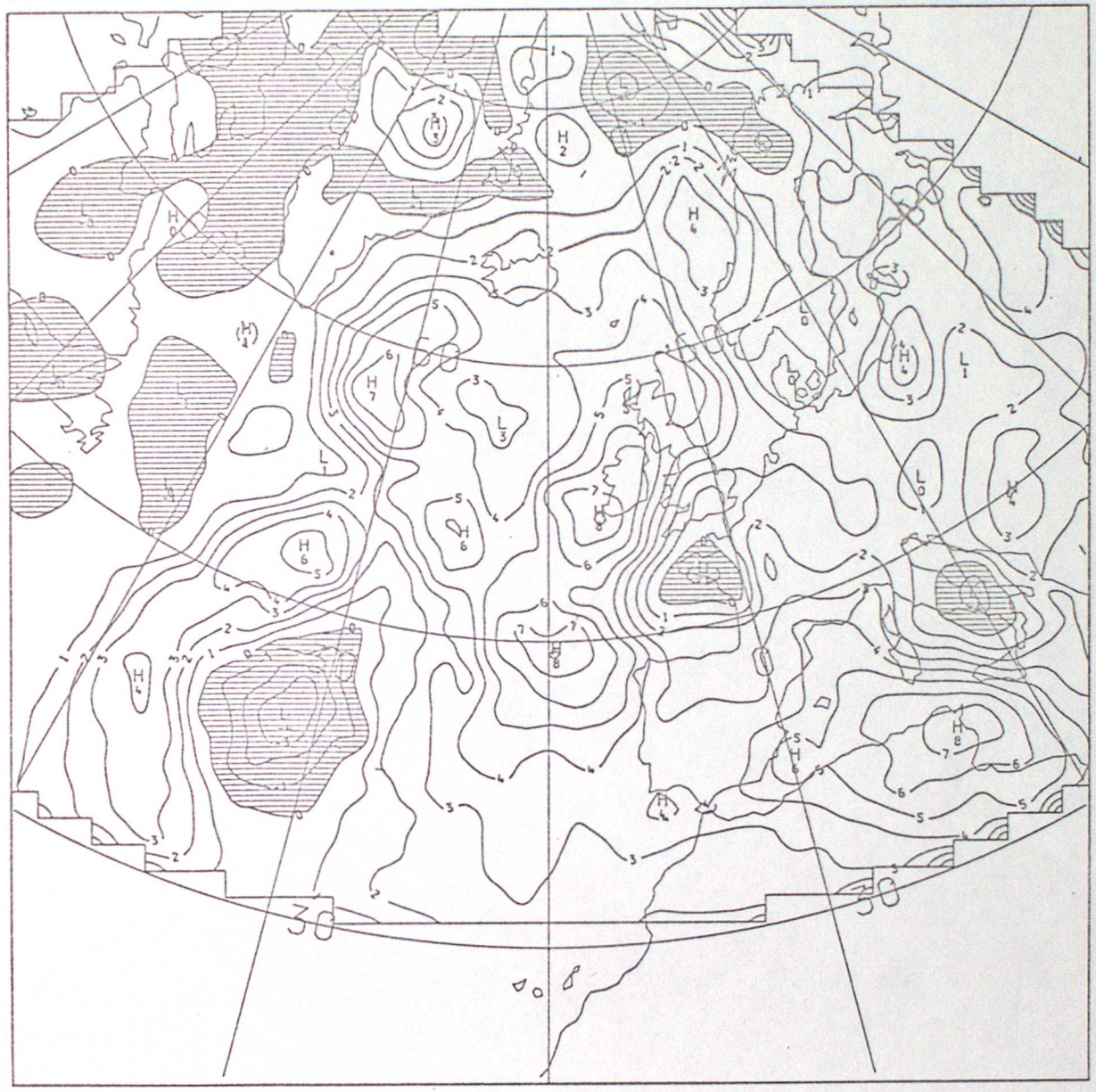

TEST1-TEST2 F.M ASSIM(HERMES MINUS CONTROL)12Z 09FEB

FIG. 14

TEMPERATURE

VALID AT 12Z ON 9/2/1984 DAY 40 DATA TIME 12Z ON 9/2/1984 DAY 40

LEVEL: 200 MB

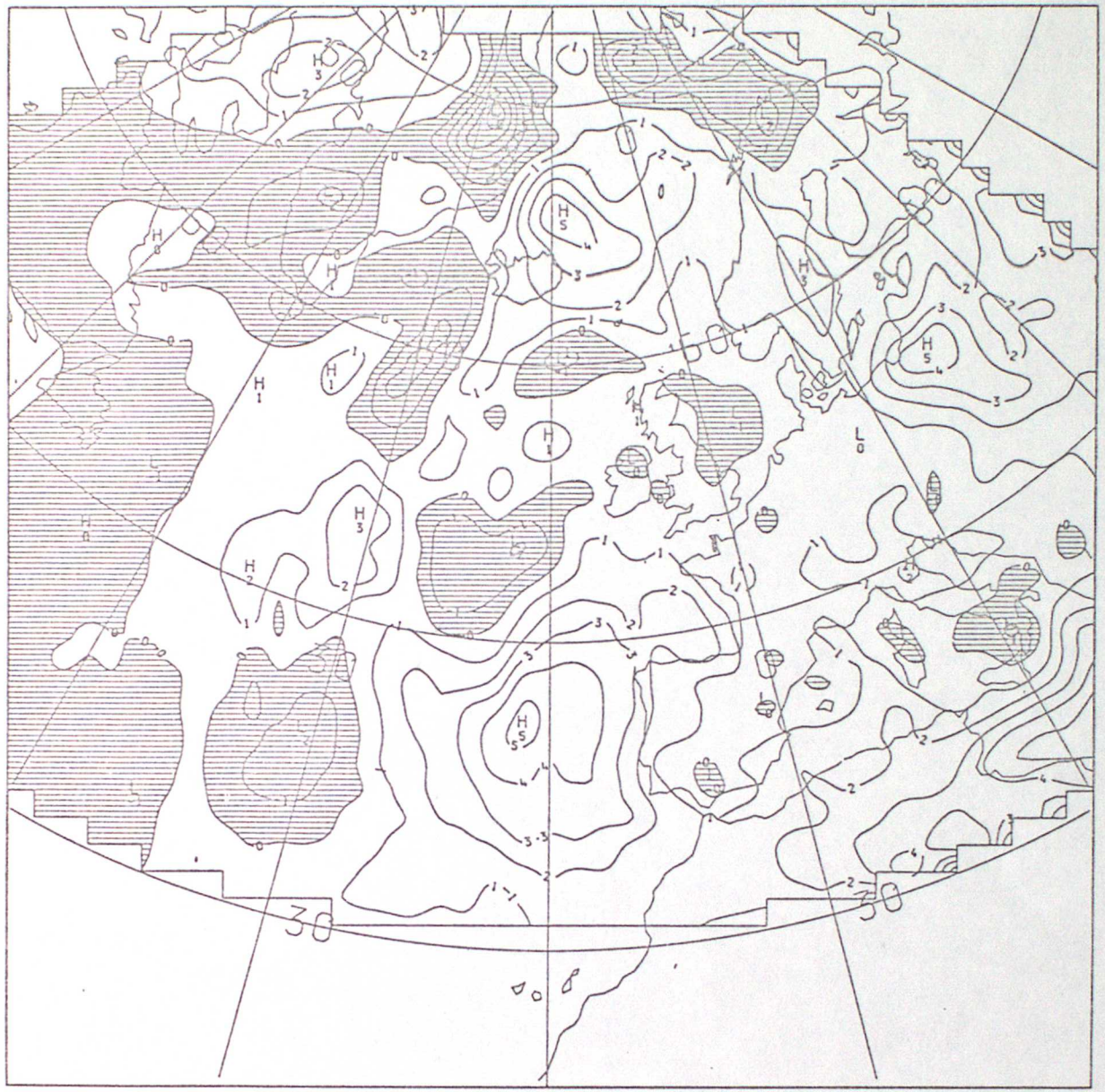

TEST1-TEST2 F.M ASSIM(HERMES(NO RS) - CONTROL)12Z 09FEB

FIG. 15

TEMPERATURE

VALID AT 12Z ON 9/2/1984 DAY 40 DATA TIME 12Z ON 9/2/1984 DAY 40

LEVEL: 200 MB

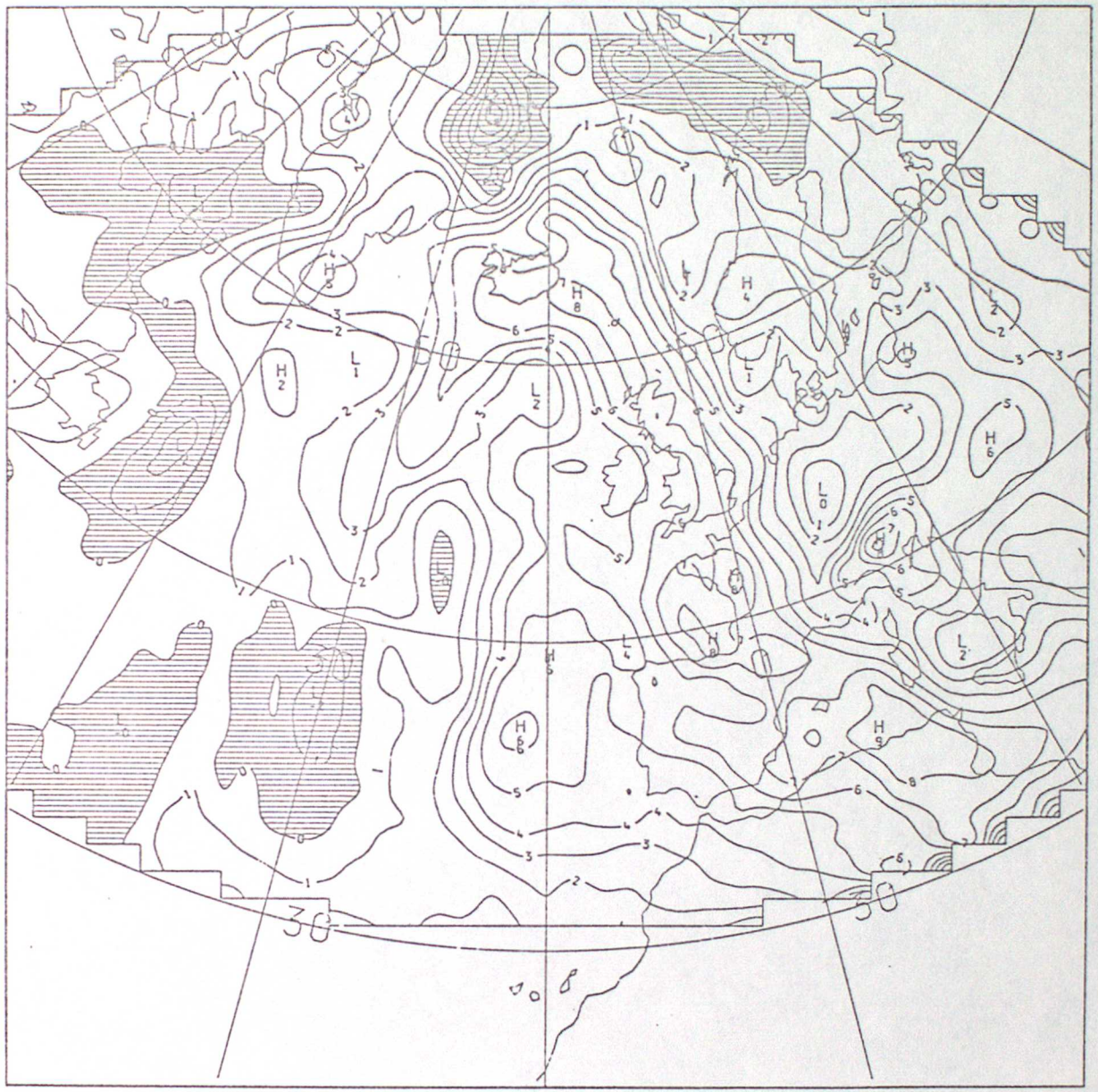

TEST1-TEST2 F.M ASSIM(HERMES - CONTROL)06Z 09FEB

FIG. 16

TEMPERATURE

VALID AT 6Z ON 9/2/1984 DAY 40 DATA TIME 6Z ON 9/2/1984 DAY 40

LEVEL: 1000 MB

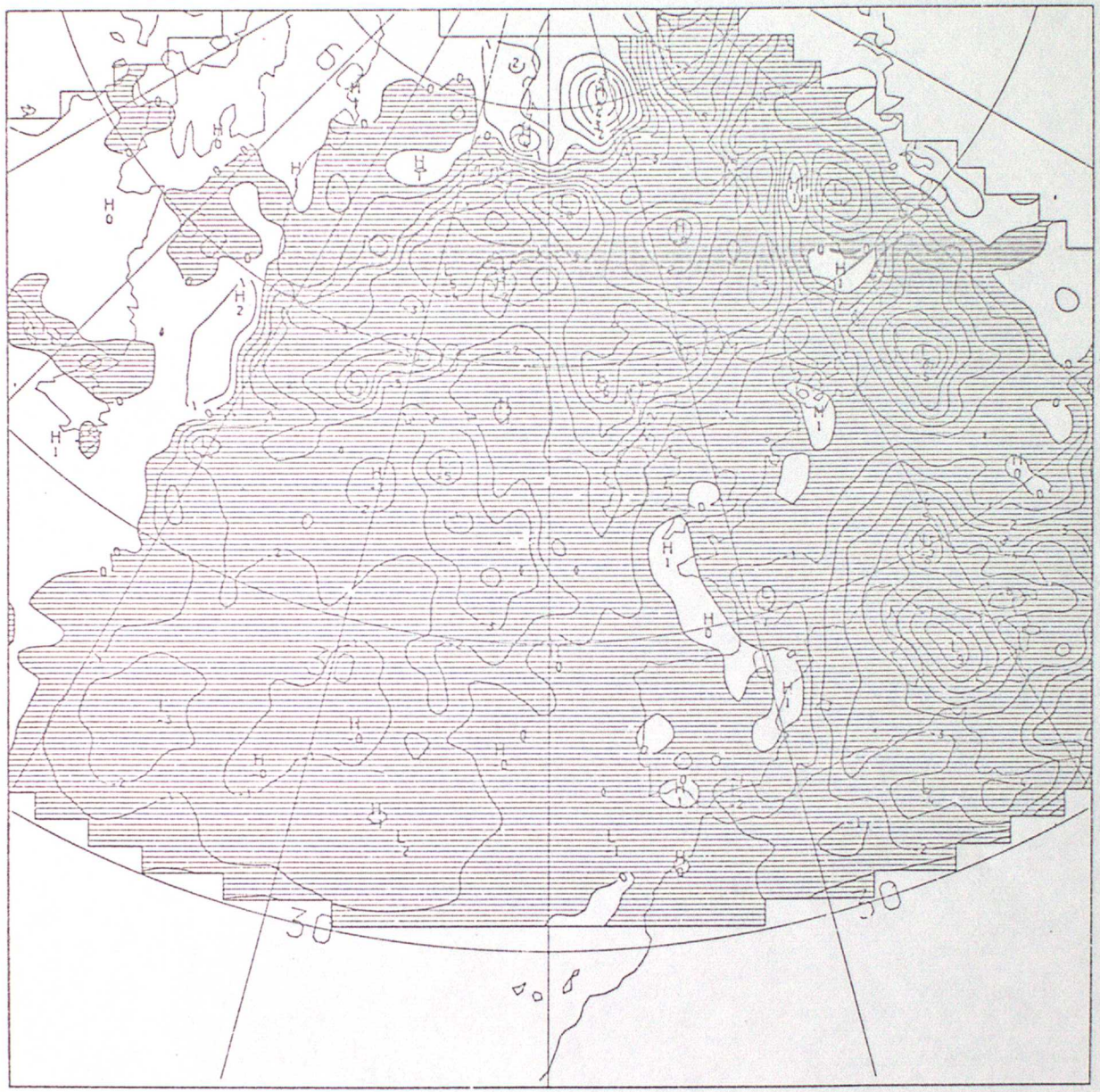

FIG. 17 a

DT 12Z 9/2/84 VT 12Z 9/2/84

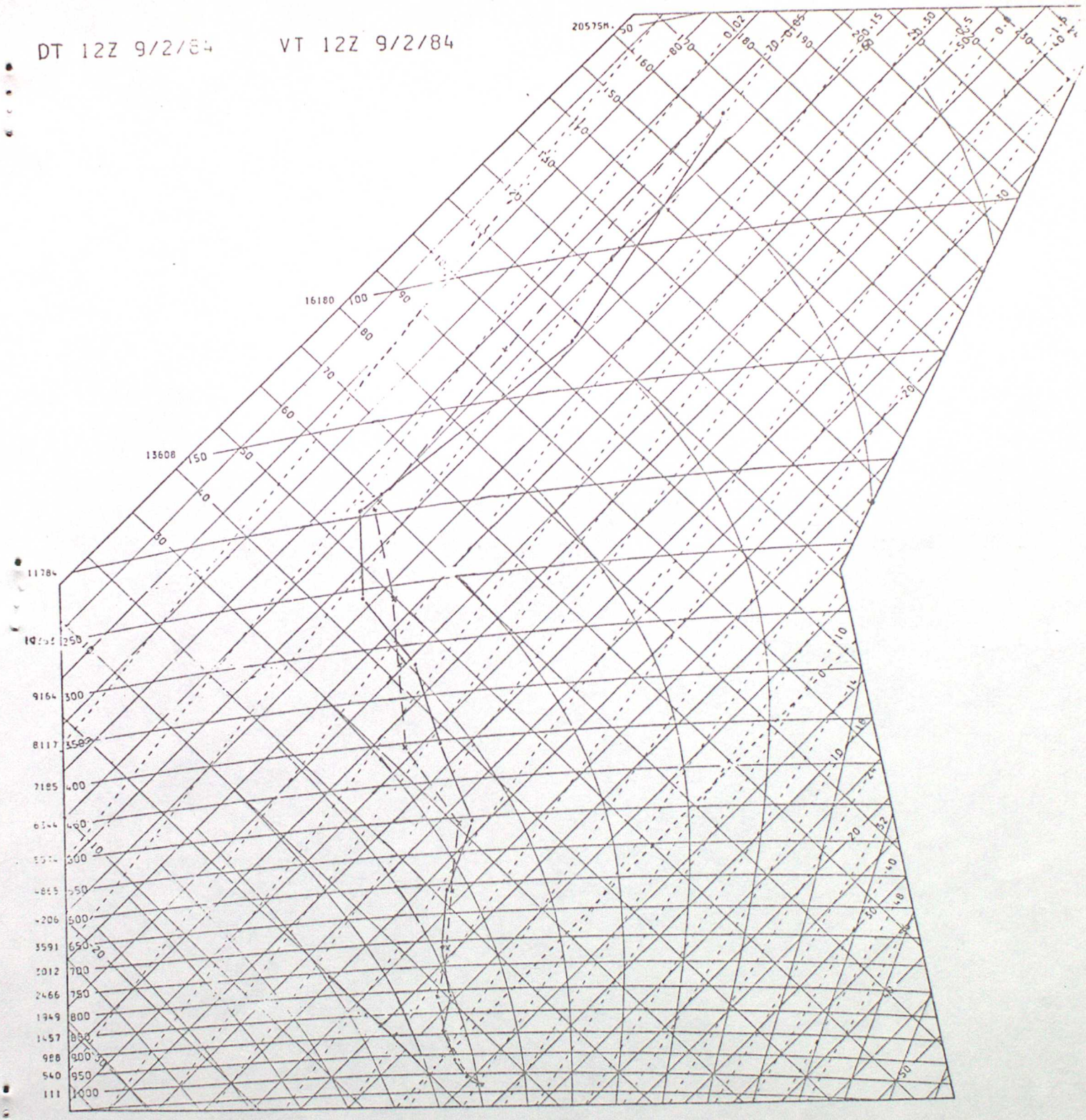

Control Background

HEMSBY (model interpretation)

FIG. 17b

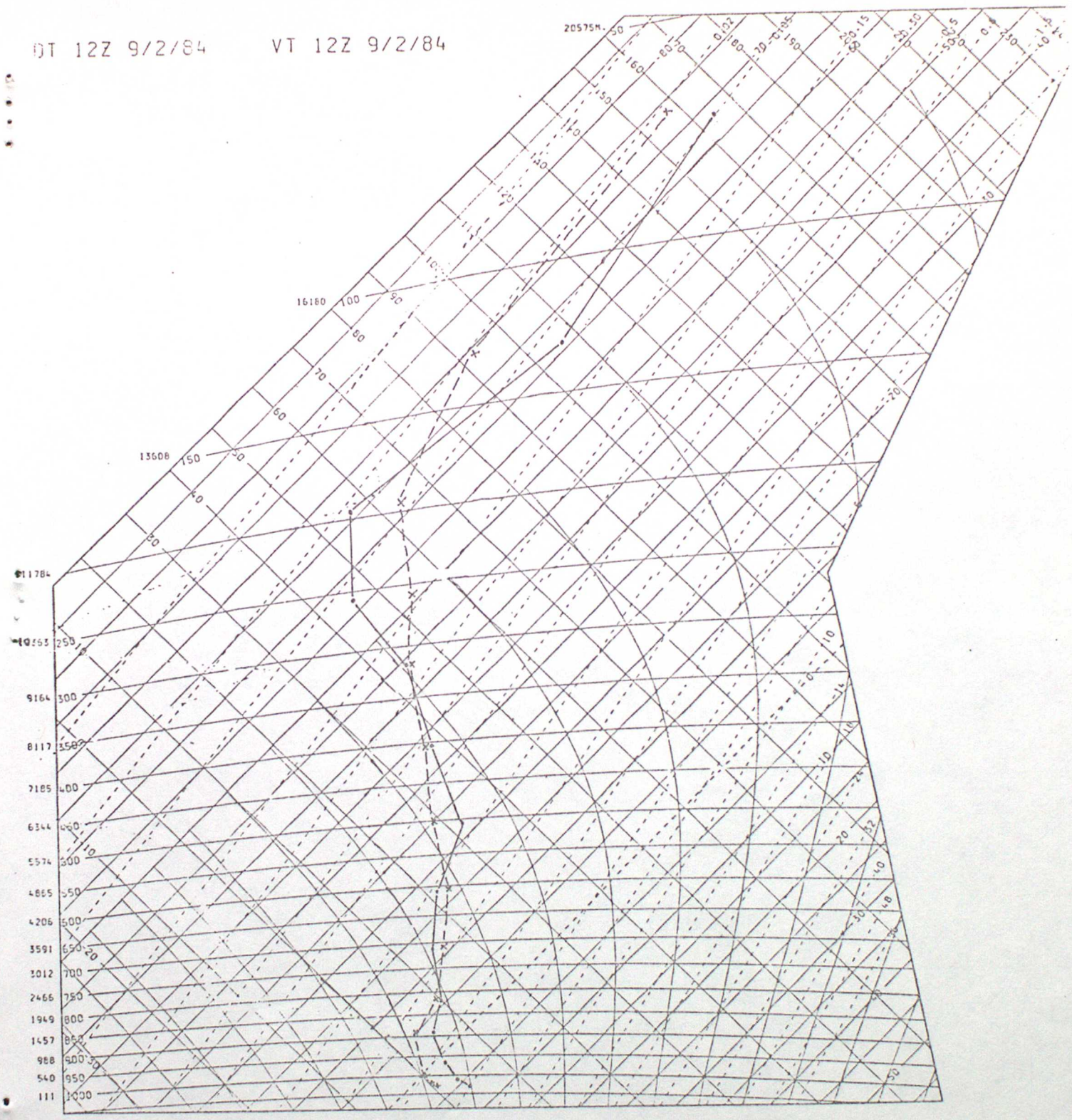

HERMES (Background)

HEMSBY (model interpretation)

FIG. 18

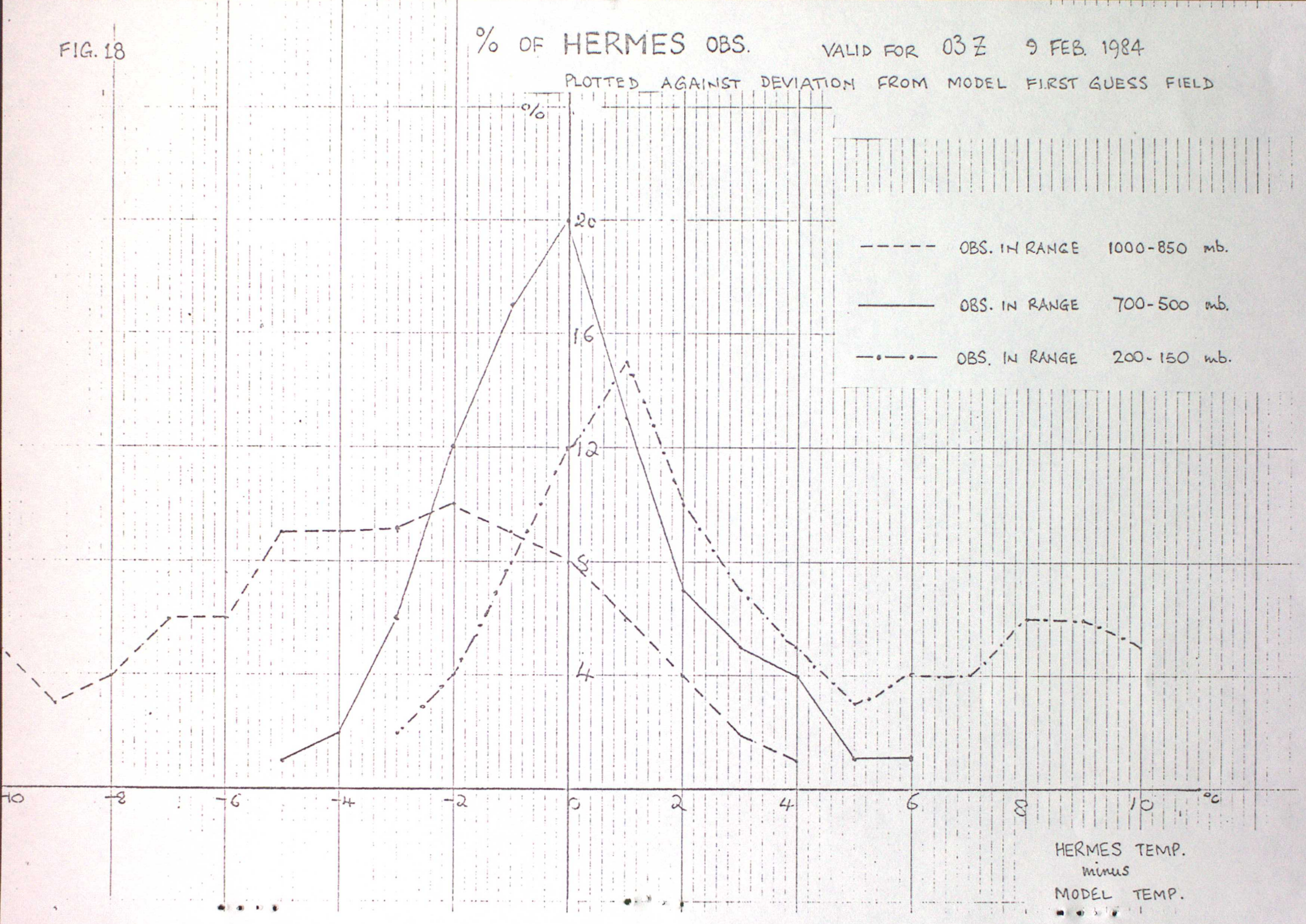
% OF HERMES OBS.
VALID FOR 03 Z 9 FEB. 1984
PLOTTED AGAINST DEVIATION FROM MODEL FIRST GUESS FIELD
%
20
16
12
8
4
OBS. IN RANGE 1000-850 mb.
OBS. IN RANGE 700-500 mb.
OBS. IN RANGE 200-150 mb.
-10
-8
-6
-4
-2
0
2
4
6
8
10
°C
HERMES TEMP.
minus
MODEL TEMP.

1000-500 THICKNESS HERMES2 MINUS NO HERMES
GEOPOTENTIAL HEIGHT
VALID AT 6Z ON 9/2/1984 DAY 40
LEVEL: 500 MB - 1000 MB

FIG. 19

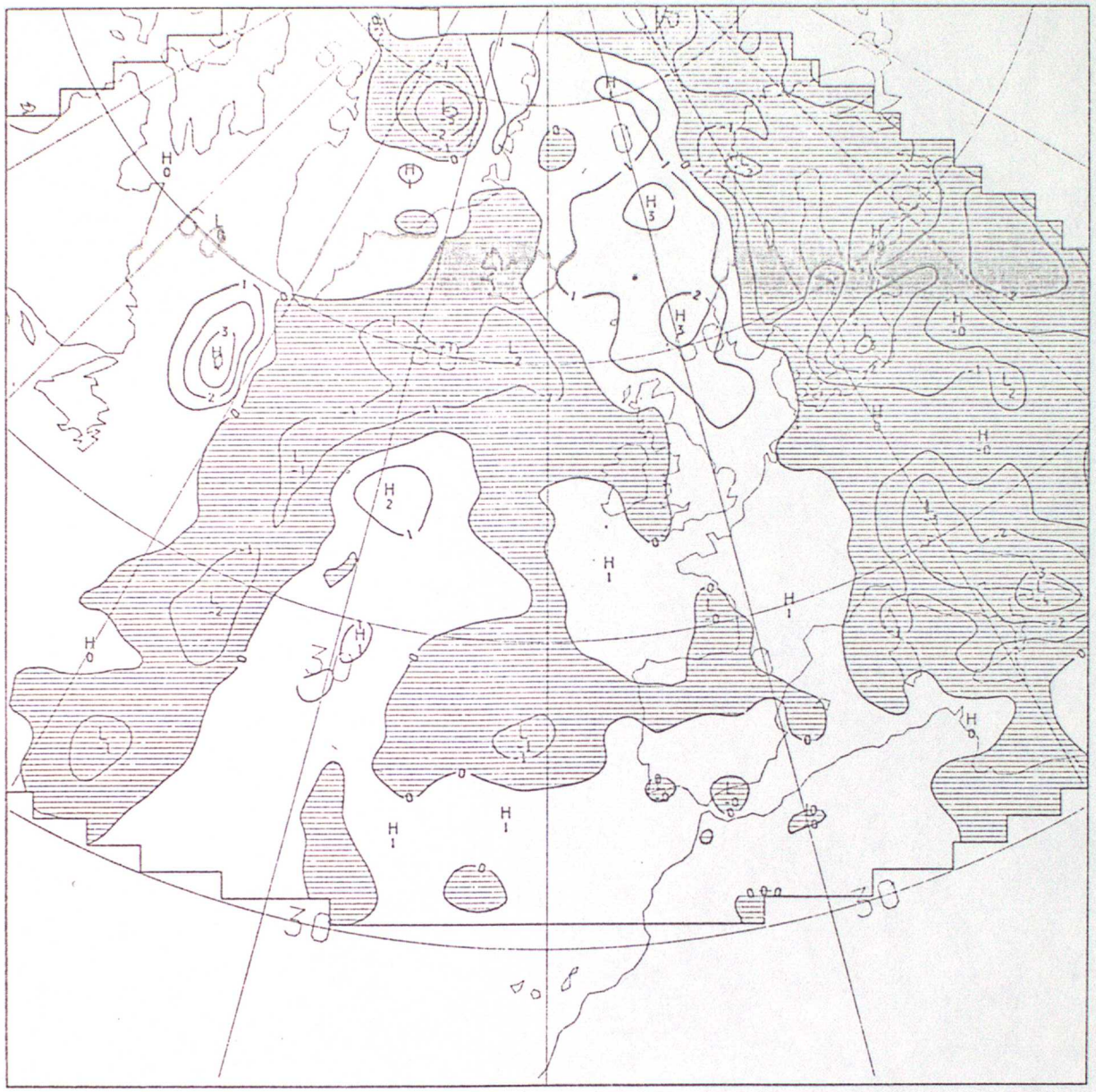

HERMES2 MINUS NO HERMES
TEMPERATURE
VALID AT 6Z ON 9/2/1984 DAY 40
LEVEL: 200 MB

FIG. 20